



ELSEVIER

European Journal of Radiology Open 1 (2014) 14–21

RADIOLOGY  
OPEN[www.elsevier.com/locate/ejro](http://www.elsevier.com/locate/ejro)

# An innovative approach to investigate the dynamics of the cerebrospinal fluid in the prepontine cistern: A feasibility study using spatial saturation-prepared cine PC-MRI

Christoph M. Rüegger<sup>a</sup>, Malek I. Makki<sup>b,\*</sup>, Cyrille Capel<sup>c</sup>,  
Catherine Gondry-Jouet<sup>d</sup>, Olivier Baledent<sup>e</sup>

<sup>a</sup> Intensive Care and Neonatology, University Hospital of Zurich, Zurich, Switzerland

<sup>b</sup> MRI Research Center, University Children's Hospital of Zurich, Zurich, Switzerland

<sup>c</sup> Department of Neurosurgery, Amiens University Hospital, Amiens, France

<sup>d</sup> Department of Radiology, Amiens University Hospital, Amiens, France

<sup>e</sup> Image Processing Unit, Amiens University Hospital, Amiens, France

Received 12 June 2014; received in revised form 29 September 2014; accepted 30 September 2014

Available online 16 October 2014

## Abstract

**Purposes:** Accurate measurements of the cerebrospinal fluid that flows through the prepontine cistern (PPC) are challenging due to artefacts originating from basilar artery blood flow. We aim to accurately quantify cerebrospinal fluid (CSF) flow and stroke volume in the PPC, which is essential before endoscopic third ventriculostomy.

**Materials and methods:** We developed a new PC-MRI sequence prepared with Hadamard saturation bands to accurately quantify CSF flow in the PPC by suppressing the blood signal in the surrounding vessels. In total, 28 adult hydrocephalic patients (age  $59 \pm 20$  years) were scanned using conventional PC-MRI and our developed sequence. CSF was separately extracted from the PPC and the foramen of Magendie, and flow (min and max) and stroke volume were quantified.

**Results:** Our modifications result in a complete deletion of signal from flowing blood, resulting in significantly reduced CSF stroke volume ( $Conv = 446 \pm 113 \text{ mm}^3$ ,  $Dev = 390 \pm 119 \text{ mm}^3$ ,  $p = 0.006$ ) and flow, both minimum ( $Conv = -1630 \pm 486 \text{ mm}^3/\text{s}$ ,  $Dev = -1430 \pm 406 \text{ mm}^3/\text{s}$ ,  $p = 0.005$ ) and maximum ( $Conv = 2384 \pm 657 \text{ mm}^3/\text{s}$ ,  $Dev = 1971 \pm 62 \text{ mm}^3/\text{s}$ ,  $p = 0.002$ ) compared with the conventional sequence, whereas no change in the area of interest was noted ( $Conv = 236 \pm 65 \text{ mm}^2$ ,  $Dev = 249 \pm 75 \text{ mm}^2$ ,  $p = 0.21$ ).

**Conclusions:** Accurate and reproducible CSF flow and stroke volume measurements in the PPC can be achieved with sat-band prepared cine PC-MRI.

© 2014 Published by Elsevier Ltd. This is an open access article under the CC BY-NC-ND license (<http://creativecommons.org/licenses/by-nc-nd/3.0/>).

**Keywords:** Prepontine cistern; Foramen of Magendie; CSF; PC-MRI; Spatial saturation; Aliasing

## 1. Introduction

Cine phase-contrast MRI (PC-MRI) is a flow-sensitive imaging method that has been increasingly used in clinical practice for quantifying blood [1] and cerebrospinal fluid (CSF)

flow [2]. CSF oscillations are altered in disorders, including hydrocephalus [3], intracranial hypo- or hypertension [4], subarachnoid haemorrhage [5], and posterior fossa cystic malformations [6]. CSF flow parameters are positively correlated with CSF opening pressure, headache scores [7], response to shunt insertion in hydrocephalic patients [3], and the success of endoscopic third ventriculostomy (ETV) in cases of aqueductal stenosis [8]. In most of these disorders, CSF dynamics are measured in the aqueduct of Sylvius and rarely in the subarachnoid spaces (SAS), although CSF flow through the SAS around the basilar artery is particularly important for brain compliance

\* Corresponding author at: University Children's Hospital of Zurich, Steinwiesstrasse 75, CH-8032 Zurich, Switzerland. Tel.: +41 (0)44 266 3130; fax: +41 (0)44 266 7153.

E-mail address: [Malek.Makki@kispi.uzh.ch](mailto:Malek.Makki@kispi.uzh.ch) (M.I. Makki).

[4,9]. Cardiac cycle (CC)-induced brain vascular expansion flushes the CSF through the spinal canal. This CSF, which oscillates during the CC, mainly originates from the intracranial SAS (90%) and to a lesser degree from the ventricular CSF (10%) [9]. This action subsequently results in an increased oscillating CSF volume in cases with decreased SAS, as noted in hydrocephalic patients or patients with subarachnoid haemorrhage [5].

Accurate CSF flow measurement with PC-MRI in general and through the PPC in particular is technically challenging. First, the CSF flows encountered are very low and therefore difficult to calculate. The error of this technique is approximately  $\pm 10\%$  when measuring flow rates through the aqueduct [10]. Background correction is required to remove the effect of phase offset errors and movement occurring during the CC [11]. Second, inappropriate selection of the maximum velocity encoding gradient (*Venc*) leads to reduced sensitivity by reducing the signal-to-noise ratio, whereas selection of lower values results in aliasing. Third, for the narrow aqueduct and PPC, the effects of limited spatial resolution cause diameter-dependent systematic overestimations in pulsatile volume changes. This problem can be resolved by increased spatial resolution at the expense of longer acquisition times and increased signal averaging [12]. Similarly, McCormac et al. noted that contrary to the laminar flows through the narrow cerebral aqueduct, CSF flow in larger regions, such as the SAS, is often turbulent. This phenomenon causes phase dispersion and signal loss in the PC-MRI, resulting in underestimation of flow in the SAS [13]. Fourth and most important, the PPC is infiltrated with the basilar artery, which generates blood flow artefacts. Surrounding vessels additionally corrupt the signal and make it difficult to segment the CSF flow area of the PPC using PC-MRI. Applying a Hanning window filter reliably reduces such artefacts but also results in a large net reduction in spatial resolution [14]. The objective of this investigation was to develop a novel 2D cine PC-MRI sequence to assess CSF dynamics that (1) is automatically filtered from blood flow artefacts at the acquisition level, (2) is highly sensitive to slow velocities typical of altered CSF dynamics and (3) does not compromise spatio-temporal resolution. We hypothesised that the saturation of the blood signal from basilar artery flow makes it possible to accurately assess CSF dynamics in the PPC. Such a CSF quantification method might be useful to better diagnose and understand various types of CSF flow alterations.

To date PC-MRI is the unique technique to assess in vivo CSF flow and dynamics despite the inheriting errors from eddy-currents, phase-shift and blood flow artefacts. Other modalities like cranial Doppler fail to achieve better results in the physiologic state because normal CSF lacks sufficient interfaces to generate signal and require presence of scattering particles or cells, thus cannot be used as a control modality. As a proof of concept, a phantom with properties optimised to resemble the properties of human SAS, PPC and FOM would be desirable. The artificial phantom used for such a validation approach would disturb the extremely sensitive and technically challenging acquisition of the PC-MRI signal and would not provide reproducible and meaningful results. Therefore, to validate our hypothesis, the foramen of Magendie (FOM) was chosen as our control structure. The FOM is not infiltrated by blood vessels;

thus, CSF flow and stroke volume measurements are unaffected by sat-pulses.

## 2. Materials and methods

### 2.1. Subjects

Twenty-eight consenting adult patients (age =  $59 \pm 20$  years, 15 females) with suspected hydrocephalus (normal pressure, idiopathic, communicating, occlusive, and secondary) were prospectively enrolled in this study. The inclusion criteria were ventricular dilation with either one of the following: gait disturbance, urinary disturbance or cognitive alterations. The patients were scanned using conventional cine PC-MRI, which is part of our routine clinical protocol for this pathology, followed by our developed sequence through the same slice position and with the same imaging parameters. The main advantage of the addition of our developed sequence to the hydrocephalus protocol is that we will perform both sequences on patients with no bias of eddy-current and/or phase-error shift. The regional ethical review board approved the study, and all participants provided written consent.

### 2.2. Image acquisition

The study was performed using a 3 T scanner (GE Healthcare) with retrospectively and peripherally gated cine PC-MRI to record 32 cardiac phases. The following imaging parameters were used: slice thickness = 5 mm, FOV = 140 mm  $\times$  140 mm, BW = 62.5 kHz, flip angle = 20°, minimum TE and TR, matrix 256  $\times$  160, and 2 views per segment. In addition, the slice position was at the level of the PPC and was obliquely oriented to be perpendicular to the direction of the CSF flow (Fig. 1). The velocity encoding (*Venc*) of the conventional sequence was set to the minimal possible value of 50 mm/s. The commercial available sequence was first modified to achieve a lower *Venc* of 20 mm/s to increase the sensitivity of the acquisition of reduced flow. In addition to removing the signal from blood flowing into the selected slice and avoiding aliases with the CSF flow signal, spatial selective pre-saturation pulses were incorporated. These pulses consisted of Hadamard pulses, or double-sided bands (20 mm thick), to achieve a perfect parallelism with the selected slice and reproduce the same sat-band (thickness, gap and orientation) in the other side. To validate our hypothesis, we oriented the slice position and the sat-bands to include both structures. On one hand, the PPC is typically infiltrated by the basilar artery and consequently suffers from blood flow artefacts. On the other hand, the FOM lacks blood flow artefact and was used as our control structure.

### 2.3. Image processing

Image processing was performed using homemade software with a dedicated CSF algorithm segmentation to differentiate tissue with reduced pulsatility compared with CSF as characterised by large amplitude oscillations and synchronised with the CC [9]. The software uses a “spectral segmentation” algorithm that

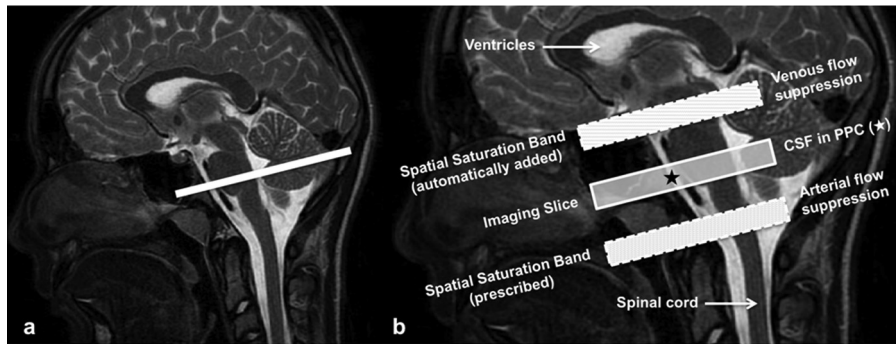


Fig. 1. Slice position through the prepontine cistern (a) and pre-saturation bands (b). One sat-band is defined in one direction, and the system automatically adjusts it to be parallel to the prescribed slice and creates an identical and symmetric sat-band with regard to the slice position. This position was set to include the PPC, which experiences blood flow artefacts that require suppression, and the FOM, which lacks artefacts and serves as a validation model.

automatically extracts a threshold value from the phase of the signal throughout the 32 cardiac phases [9]. An automatic and separate delineation of CSF in the PPC and FOM (Fig. 2) was performed to extract the velocity in each compartment through each of the 32 cardiac phases. CSF oscillation with the cardiac cycle consists of 2 parts: the caudo-cranial flow (minimum negative value) and the cranio-caudal flow (maximum positive value). Minimum and maximum CSF flows, stroke volume and ROI area were measured, and the values obtained by the *Conv* and *Dev* sequences were compared. Stroke volume, expressed in  $\mu\text{l}/\text{CC}$ , was defined as the average of the cranio-caudal and caudo-cranial volumes displaced through the region of interest during the CC. Intra- and inter-observer reliability (2 observers) were assessed using interclass correlation coefficients ( $ICC > 0.8$  excellent reliability), whereas the difference between *Conv* and *Dev* was assessed using a paired *t*-test ( $p < 0.05$  is considered significant).

### 3. Results

#### 3.1. Blood saturation

Using conventional cine PC-MRI, blood flowing through the basilar artery always generates aliases due to a considerably higher velocity than the CSF not only within the PPC but also in

surrounding vessels (Fig. 3). In addition, with a  $V_{enc} = 50 \text{ mm/s}$ , the phase images exhibit very low contrast between the FOM and the surrounding tissues. The first advantage of incorporating spatial saturation pulses is clearly demonstrated by a complete suppression of the blood signal not only within the PPC but also in other small vessels (Fig. 3). Furthermore, by implementing a lower  $V_{enc}$  (20 mm/s), the FOM is clearly highlighted in the phase images.

#### 3.2. Interclass correlation coefficient

The minimum ICC for the intraclass correlation (28 patients) was reported in the area of the PPC (Table 1) for both sequences (0.78 for *Conv* and 0.92 for *Dev*). An interclass correlation test was performed (18 randomly selected patients), and the ICC in the PPC ranged from 0.80 for the flow minimum with *Conv* to 0.96 for the stroke volume with *Dev*. In the FOM, the ICC coefficient ranged from 0.78 for the ROI to 0.90 for the stroke volume (Table 1).

#### 3.3. Conventional versus developed

The background phase offset errors were minimised by drawing an ROI on static tissue and subtracting the signal intensity for each cardiac phase for the two sequences (*Conv* and *Dev*).

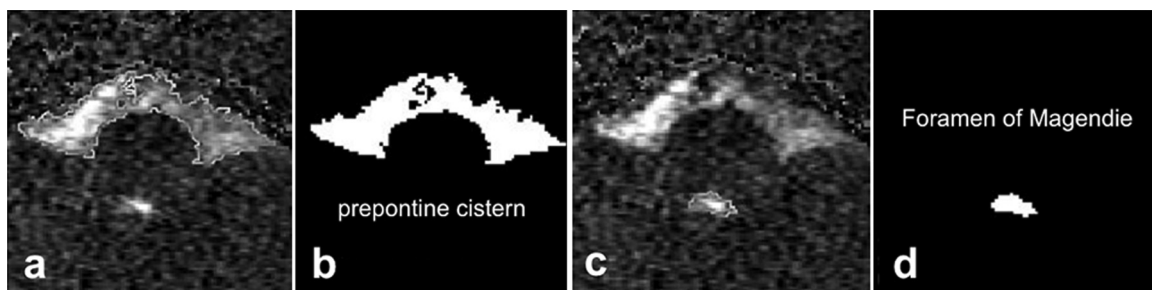


Fig. 2. The result of the semi-automatic segmentation: (a) prepontine cistern delineation, (b) prepontine cistern mask revealing blood flow artefacts (dark pixels from the basilar artery), (c) delineation of the foramen of Magendie (lacks artefacts given that there are no vessels in or around the structure) and (d) the resulting mask. The mask areas are used to compare the developed sequence to the conventional sequence. In addition, the flow through these areas is measured for each cardiac cycle and compared.

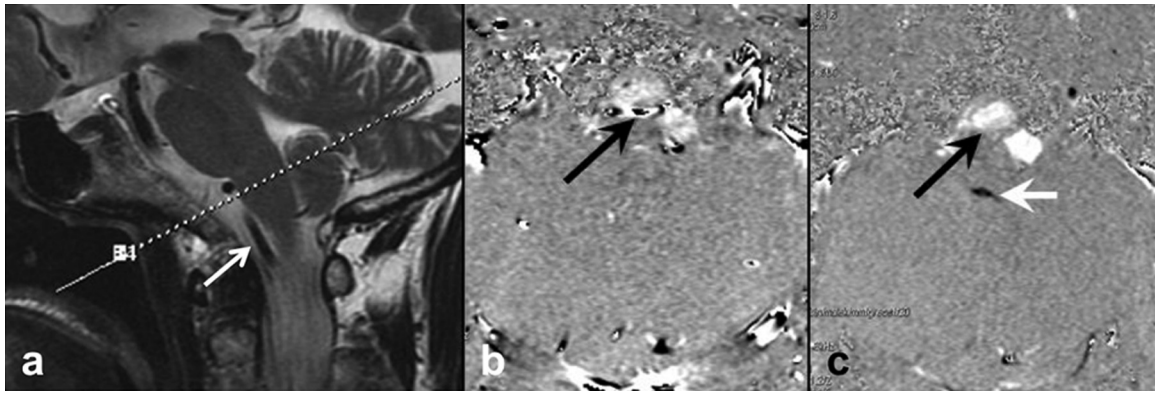


Fig. 3. (a) The basilar trunk (white arrow) observed on a T2W image (b) generates artefacts in the prepontine cistern (PPC) represented by an aliasing of the signal (black arrow) with a conventional cine PC-MRI. The advantage of the developed sequence is clearly demonstrated (c) with the incorporation of saturation bands to negate the signal from flowing blood (black arrow). Furthermore, by reducing the  $V_{enc}$  to 20 mm/s, the foramen of Magendie appears with good contrast and can be segmented easily (white arrow).

Table 1

Inter and intra raters correlation coefficient values for the stroke volume, flow (min = minimum and max = maximum) and area of the prepontine cistern (PPC) and foramen of Magendie (FOM). Inter-rater was carried out on all processed 28 patients, while the intra-rater was performed on randomly selected 18 patients.

ICC	Stroke volume		Flow (min)		Flow (max)		Area	
	Inter	Intra	Inter	Intra	Inter	Intra	Inter	Intra
FOM								
Conventional	0.85	0.94	0.84	0.98	0.86	0.96	0.85	0.92
Developed	0.90	0.99	0.89	0.99	0.91	0.99	0.78	0.97
PPC								
Conventional	0.90	0.92	0.92	0.98	0.80	0.95	0.87	0.78
Developed	0.96	0.99	0.95	0.99	0.96	0.98	0.93	0.92

Temporal analysis per CC versus the PPC flow curve indicated that the negative peak values were almost identical (approximately 4% difference) for both sequences, *Conv* ( $-1331 \pm 623 \text{ mm}^3/\text{s}$ ) and *Dev* ( $-1272 \pm 360 \text{ mm}^3/\text{s}$ ). An

approximate 20% difference in the positive peak values was noted, with amplitudes of  $+2028 \pm 593 \text{ mm}^3/\text{s}$  for *Conv* compared with  $1600 \pm 526 \text{ mm}^3/\text{s}$  for *Dev* (Fig. 4a). We also observed that *Dev* is slightly shifted to the left side ( $\sim 1$

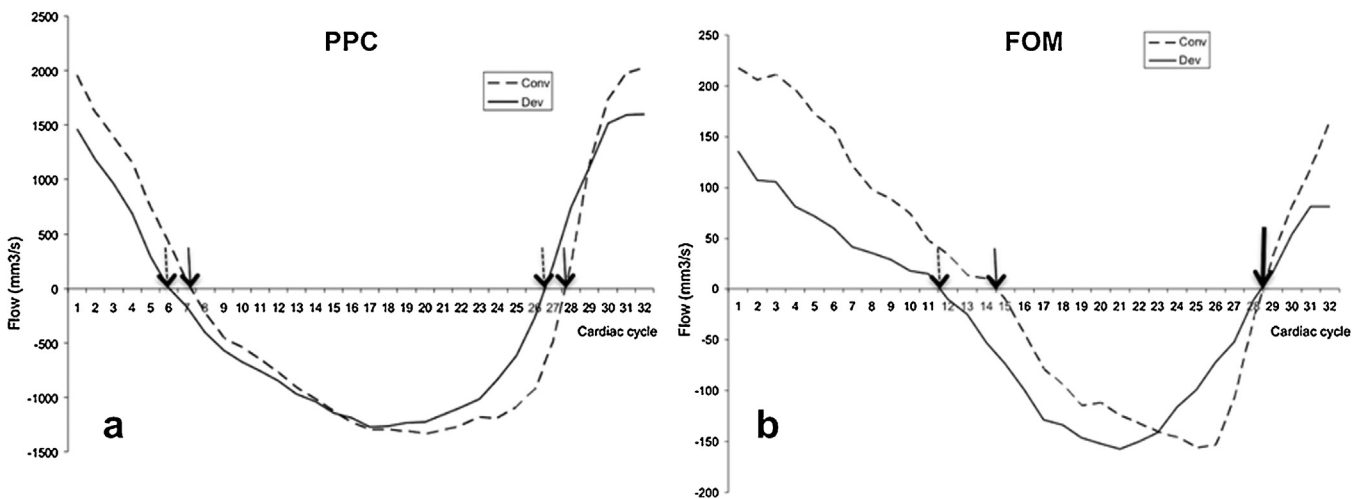


Fig. 4. Average flow curves of the 28 patients demonstrate similar patterns as well as similar negative peak values in (a) the prepontine cistern (PPC) and (b) the foramen of Magendie (FOM). We also observed a shift towards left-hand side with the developed sequence (*Dev*) compared with the conventional sequence (*Conv*). The shift is approximately 1 phase in the PPC ( $\sim 23 \text{ ms}$ ) and 3 phases in the FOM ( $\sim 70 \text{ ms}$ ); however, no effects on the diastolic or systolic periods are observed. The maximum positive peaks differ between the two sequences for both the FOM and PPC. The ratio systole/diastole was 12/20 phases for both sequences in the PPC. In the FOM, this ratio was approximately 13/19 using the *Conv* sequence and 16/16 using the *Dev* sequence.

phase of the CC,  $\sim 23$  ms), but neither the systolic nor the diastolic period differed when we compared the 2 sequences ( $p = 0.349$ ). Similarly, in the FOM, we recorded an approximate 6% difference in the negative maximum flow values between *Conv* ( $-148 \pm 191$  mm<sup>3</sup>/s) and *Dev* ( $-157 \pm 163$  mm<sup>3</sup>/s), whereas the positive peak flow differed by approximately 25% ( $184 \pm 247$  mm<sup>3</sup>/s and  $+136 \pm 166$  mm<sup>3</sup>/s, respectively) (Fig. 4b). We also report a shift in *Dev* towards earlier CCs ( $\sim 3$  phases,  $\sim 70$  ms) compared with *Conv*, but neither the diastolic nor the systolic period significantly differed when comparing the 2 sequences ( $p = 0.127$ ).

With regard to the *Dev* sequence, no significant difference in the area of the PPC was observed (Table 2); however, a significantly lower stroke volume ( $p = 0.006$ ) and lower flow (minimum  $p = 0.002$  and maximum  $p = 0.005$ ) were observed compared with the *Conv* sequence (Fig. 5). In contrast, the area in the FOM (Table 2) was significantly increased ( $p < 0.001$ ) in *Dev* with no effect on stroke volume or flow minimum. However, a significantly increased maximum flow was noted with *Dev* ( $p = 0.004$ ).

A Pearson test between stroke volume and area of interest as well as flow maximum and area of interest was performed in the PPC and FOM to assess the correlation with *Dev* (Fig. 5). In the FOM, we measured approximately the same correlation coefficients with *Conv* and *Dev* for the flow maximum as well as the stroke volume. In the PPC, we observed a slightly increased correlation for the stroke volume and flow maximum with *Dev* compared with *Conv*.

#### 4. Discussion

A Hadamard double saturation-bands cine PC-MRI sequence was developed and applied to investigate the complex dynamics of cerebral CSF in the PPC caused by aliasing the signal from blood flowing in the basilar artery and surrounding vessels. We investigated this phenomenon at the acquisition level to avoid offline processing and preserve both temporal and spatial resolutions. The main findings are consistent with our hypothesis based on the following observations in the PPC: (1) flowing blood signal saturation and alias removal were achieved; (2) a significantly reduced stroke volume and flow, minimum and maximum, compared with that of the conventional sequence were obtained; and (3) no difference in the surface of the selected region was noted.

Qualitative analysis of the phase images clearly demonstrates that the aliased pixels from blood flowing in the basilar artery observed with *Conv* (dark pixels within PPC) were recovered with *Dev* (bright pixel) in these patients. In fact, our *Dev* does not change the number of pixels only the pixel content. As a consequence, outlier pixels, which represent flowing blood at velocity of  $> 50$  mm/s, exhibit saturated signals and do not contribute to the overall signal.

In addition, with a lower *Venc* (20 mm/s), the enhanced phase signal in the FOM allows enhanced extraction of this structure and hence reduces the inaccuracy that results from partial volume and the increased sensitivity to slow flow with such a low *Venc*. The reliability and reproducibility of *Dev* compared with

*Conv* were demonstrated by enhanced correlation of the flow in the area of interest in the PPC. With regard to the FOM, although the ROI area was significantly different ( $p < 0.001$ ), the CSF flow and stroke volume were unaffected. This finding is consistent with our hypothesis that the added sat-pulses increase the number of pixels but have no effect on pixel content; thus, the measurements of flow, velocity and stroke volume are unaffected because there are no vessels in and around the FOM. One can conclude that partial volume effects and high *Venc* ( $> 20$  mm/s) generate substantial errors in the measurements of CSF parameters in the FOM when no correction is performed with *Conv*. Second, suppression of the aliasing signal within the internal pixels of this structure with our *Dev* provides the correct velocity, which is translated to the phase images by the flow encoding gradients.

The temporal analysis of the CSF waveform at the level of the PPC exhibits similar patterns for both sequences. The systole lasts for 12 phases ( $\sim 280$  ms), whereas the diastole lasts for 20 phases ( $\sim 468$  ms), thereby accounting for 37% and 63%, respectively, of the cardiac cycle. A slight leftward shift of the flow curve was noted with *Dev* such that both the diastole and systole start and end earlier than with *Conv*. We conclude that the added sat-pulses do not influence the chronologic occurrence of the 2 periods during the cardiac phases in the PPC but rather influence the magnitude of these measures. In the FOM, we recorded a longer systole using *Conv*, approximately 19 phases (444 ms,  $\sim 59\%$ ) than diastole, approximately 13 phases (304 ms,  $\sim 41\%$ ). Using *Dev*, the diastole and systole periods are identical with 16 cardiac phases each ( $\sim 374$  ms). However, we noticed an early start of the diastole (leftward shift  $\sim 70$  ms) using *Dev* compared with *Conv*. Interestingly, the diastole periods end at the same time for both sequences. This shift might be explained by a partial volume effect (more pixels are included in the ROI), reducing the *Venc* to 20 mm/s (more sensitivity to slow flow), or the time required by the sat-pulse. It is important to note that the enlargement of the diastole does not affect the overall volume measurements (time integral) in the FOM given the smaller flow magnitude.

To remedy to signal aliasing and partial volume artefacts, various semi-automated [10,15] and manual [12] segmentation algorithms were developed to define the cisternal ROI. Numerous algorithms were applied to correct for errors in visually detected aliased pixels exhibiting either lower or higher velocity than the prescribed *Venc* [9]. These processes were designed to minimise errors depicted in pixels by doubling the *Venc* [16] but cannot overcome aliasing for blood pixels flowing at *Venc*  $> 800$  mm/s. Thus, using *Dev* to saturate the blood signal and avoid aliasing prior to image acquisition is of great interest for clinical application and might explain the high incidence of ETV failure. Although the offline techniques are applied as routines for quantification of volumetric CSF flow, only one of these techniques delineated and extracted blood flow artefacts within the CSF signal [12]. However, this manual offline image processing approach is subjective, imprecise and time consuming, especially for narrow structures, such as the cerebral aqueduct and complex dynamic observed in the PPC. Furthermore, ICC values were equal to or less than 0.85; this finding is most likely

Table 2

The results of paired *t*-test between the conventional sequence and the developed one that demonstrates the differences when measuring the stroke volume, the flow (min = minimum, max = maximum) and the area of interest in the prepontine cistern (PPC) and foramen of Magendie (FOM). The significance of the threshold value was set to 0.05 (NS = not significant). The + sign (respectively -) in the parentheses means higher (respectively lower) value in *Dev* compared with *Conv*. Average raw data are given with  $\pm$  standard deviation.

	Foramen of Magendie			Prepontine cistern		
	<i>Conv</i>	<i>Dev</i>	<i>p</i>	<i>Conv</i>	<i>Dev</i>	<i>p</i>
Stroke volume (mm <sup>3</sup> )	55 $\pm$ 65	41 $\pm$ 44	NS	446 $\pm$ 113	390 $\pm$ 117	0.006 (-)
Flow max (mm <sup>3</sup> /s)	30 $\pm$ 15	191 $\pm$ 192	0.004 (+)	2384 $\pm$ 657	1971 $\pm$ 62	0.002 (-)
Flow min (mm <sup>3</sup> /s)	-212 $\pm$ 217	183 $\pm$ 175	NS	-1630 $\pm$ 486	-1430 $\pm$ 406	0.005 (-)
Area (mm <sup>2</sup> )	19 $\pm$ 15	26 $\pm$ 16	<0.001 (+)	236 $\pm$ 65	249 $\pm$ 75	NS

due to the manual segmentation used in that study. Using the automatic procedure to separately extract the ROI, our novel PC-MRI sequence exhibits accurate and reproducible CSF flow and stroke volume measurements in the PPC. These features could potentially impact the diagnosis and understanding of various types of CSF flow alterations particularly in patients with obstructive hydrocephalus for which an unimpaired CSF flow to the basal cisterns is crucial and requires a separate investigation. It has been demonstrated that CSF flow imaging is a fast tool for pre- and postoperative functional evaluation of third ventriculostomy [17]. This evaluation is more important in younger patients for whom clinical signs and symptoms of

hydrocephalus may be difficult to diagnose before it reaches critical stages [18]. To date, a range of CSF flow image parameters, including ventricular size and the CSF stroke volume in the third ventriculostomy, aqueduct and basal cisterns, have been assessed to evaluate the success of ETV [19,20]. None of these parameters are reliably useful in differentiating between successful and failed ETV groups. Di et al. hypothesised that weakened CSF pathways beyond basal cisterns around the brain stem and cervical medullar junction might play an essential role in achieving ETV success [21], thereby resulting in CSF flow velocity and volume measurements in the PPC. Similarly, other authors demonstrated that although CSF flow

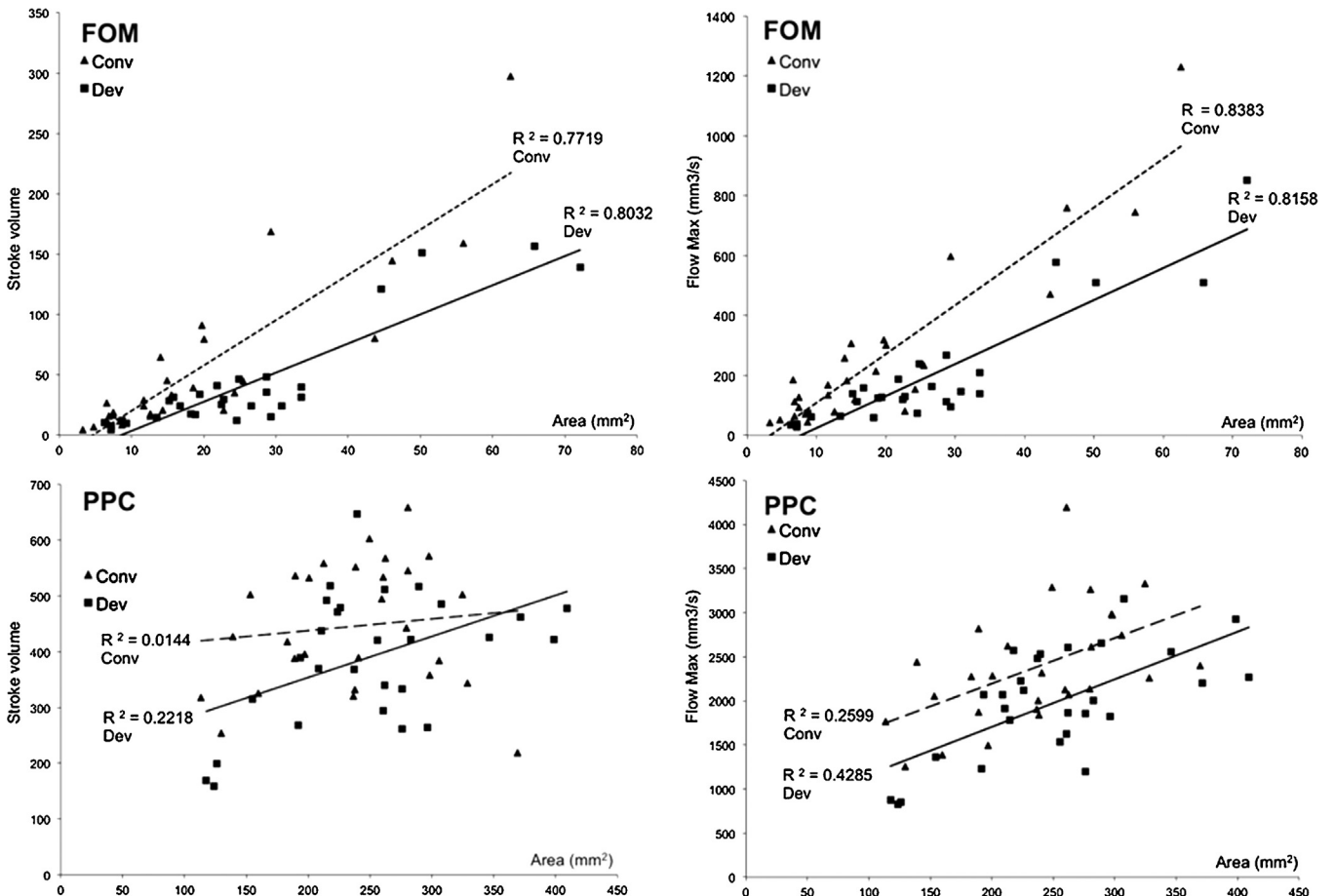


Fig. 5. Linear correlations of stroke volume with the area of interest in the foramen of Magendie (FOM) and prepontine cistern (PPC). These assessments were performed for both sequences to compare the reliability of the developed sequence.

in the stoma is useful for defining an intact and function ventriculostomy, the CSF flow measurement obtained from the PPC could be deteriorated [8]. These results suggest that CSF stroke volume and velocity at the interpeduncular cistern might predict the success of ETV. Despite obstructions at various levels caused by anatomic structures, such as membranes and aliasing artefacts from flowing blood, CSF flow signal in the prepontine area affects PC-MRI measurements. Given that our developed sequence exhibited significantly lower positive peak values, stroke volumes and flows compared with *Conv*, it raises the question as to whether CSF flow at the PPC level has been overestimated to date, thereby resulting in false negative results concerning ETV success. Our reduced correlation between the *Conv* and *Dev* sequences in the PPC might be explained by a higher sensitivity and greater accuracy when decreasing *Venc* to 20 mm/s and also a more precise delineation of CSF flow regions free of blood flow artefact [14].

The advantage of our developed sequence was validated in patients with suspected hydrocephalus based on the following reasons: (1) we were able to achieve a straight and immediate comparison with conventional PC-MRI, which is a component of the daily clinical protocol for this category of patients; and (2) this specific pathology (either normal pressure, obstructive, or communicating) presents an irregular and wider range of CSF oscillations in both the PPC and the FOM compared with healthy controls (Fig. 5). This large window of pathological hydrocephalus-related values is more challenging and provides a better assessment of the robustness in such a difficult pathology and complex CSF dynamics. Our next aim is to apply this technique to a healthy control population and define the normal physiological values of CSF in the PPC.

## 5. Conclusion

Our hypothesis regarding the assessment of CSF flow free of blood signal artefact using a PC-MRI sequence with blood saturation pulses was examined in the FOM and the PPC. This feasibility study revealed no differences in CSF dynamics in the FOM. However, significantly reduced flow and stroke volume were observed in the PPC because these measurements are affected by blood flow artefacts from surrounding vessels. The new sequence has the potential to result in a better diagnosis of CSF disorders in the PPC. Future studies involving follow-up of patients with altered CSF circulation who require surgical intervention, such as a shunt or ETV, will demonstrate the advantage of PC-MRI with sat-pulses.

## Conflict of interest

None declared.

## Acknowledgement

C.R. was supported by a Swiss National Science Foundation (SNSF) Career Award for Medical Scientists (33CM30.140334).

## References

- [1] Enzmann DR, Ross MR, Marks MP, Pele NJ. Blood flow in major cerebral arteries measured by phase-contrast cine MR. *AJNR Am J Neuroradiol* 1994;15:123–9.
- [2] Balédent O, Gondry-Jouet C, Stoquart-Elsankari S, Bouzerar R, Le Gars D, Meyer ME. Value of phase contrast magnetic resonance imaging for investigation of cerebral hydrodynamics. *J Neuroradiol* 2006;33:292–303.
- [3] Bradley WG, Scalzo D, Queralt J, Nitz WN, Atkinson DJ, Wong P. Normal-pressure hydrocephalus: evaluation with cerebrospinal fluid flow measurements at MR imaging. *Radiology* 1996;198:523–9.
- [4] Tain RW, Bagci AM, Lam BL, Sklar EM, Ertl-Wagner B, Alperin N. Determination of cranio-spinal canal compliance distribution by MRI: methodology and early application in idiopathic intracranial hypertension. *J Magn Reson Imaging* 2011;34:1397–404.
- [5] Saliou G, Paradot G, Gondry C, Bouzerar R, Lehmann P, Meyers ME, et al. A phase-contrast MRI study of acute and chronic hydrodynamic alterations after hydrocephalus induced by subarachnoid hemorrhage. *J Neuroimaging* 2012;22:343–50.
- [6] Yildiz H, Yazici Z, Hakyemez B, Erdogan C, Parlak M. Evaluation of CSF flow patterns of posterior fossa cystic malformations using CSF flow MR imaging. *Neuroradiology* 2006;48:595–605.
- [7] Hasiloglu Z, Albayram S, Gorucu Y, Selcuk H, Cagil E, Erdemli HE, et al. Assessment of CSF flow dynamics using PC-MRI in spontaneous intracranial hypotension. *Headache* 2012;52:808–19.
- [8] Anik I, Etus V, Anik Y, Cylan S. Role of interpeduncular and prepontine cistern cerebrospinal fluid flow measurements in prediction of endoscopic third ventriculostomy success in pediatric triventricular hydrocephalus. *Pediatr Neurosurg* 2010;46:344–50.
- [9] Balédent O, Henry-Feugeas MC, Idy-Peretti I. Cerebrospinal fluid dynamics and relation with blood flow: a magnetic resonance study with semiautomated cerebrospinal fluid segmentation. *Invest Radiol* 2001;36:368–77.
- [10] Yoshida K, Takahashi H, Saijo M, Ueguchi T, Tanaka H, Fujita N, et al. Phase-contrast MR studies of CSF flow rate in the cerebral aqueduct and cervical subarachnoid space with correlation-based segmentation. *Magn Reson Med* 2009;8:91–100.
- [11] Gatehouse PD, Rolf MP, Graves MJ, Hofman MB, Totman J, Werner B. Flow measurement by cardiovascular magnetic resonance: a multi-centre multi-vendor study of background phase offset errors that can compromise the accuracy of derived regurgitant or shunt flow measurements. *J Cardiovasc Magn Reson* 2010;12:5.
- [12] Wählin A, Ambarki K, Hauksson J, Birgander R, Malm J, Eklund A. Phase contrast MRI quantification of pulsatile volumes of brain arteries, veins, and cerebrospinal fluids compartments: repeatability and physiological interactions. *J Magn Reson Imaging* 2012;35:1055–62.
- [13] McCormack EJ, Egnor MR, Wagshul ME. Improved cerebrospinal fluid flow measurements using phase contrast balanced steady-state free precession. *Magn Reson Imaging* 2007;25:172–82.
- [14] Lagerstrand KM, Vikhoff-Baaz B, Starck G, Forssell-Aronsson E. Quantitative phase-contrast flow MRI measurements in the presence of a second vessel closely positioned to the examined vessel. *J Magn Reson Imaging* 2006;23:156–62.
- [15] Hamilton R, Dye J, Frew A, Baldwin K, Hu X, Bergsneider M. Quantification of pulsatile cerebrospinal fluid flow within the prepontine cistern. *Acta Neurochir Suppl* 2012;114:191–5.
- [16] Henk CB, Grampp S, Koller J, Schoder M, Frank H, Klaar U, et al. Elimination of errors caused by first-order aliasing in velocity encoded cine-MR measurements of postoperative jets after aortic coarctation: in vitro and in vivo validation. *Eur Radiol* 2002;12:1523–31.
- [17] Hoffmann KT, Lehmann TN, Baumann C, Felix R. CSF flow imaging in the management of third ventriculostomy with a reversed fast imaging with steady-state precession sequence. *Eur Radiol* 2003;13:1432–7.

- [18] Fischbein NJ, Ciricillo SF, Barr RM, McDermott M, Edwards MS, Geary S, et al. Endoscopic third ventriculocisternostomy: MR assessment of patency with 2-D cine phase-contrast versus T2-weighted fast spin echo technique. *Pediatr Neurosurg* 1998;28:70–8.
- [19] Lev S, Bhadelia RA, Estin D, Heilman CB, Wolpert SM. Functional analysis of third ventriculostomy patency with phase-contrast MRI velocity measurements. *Neuroradiology* 1997;39:175–9.
- [20] Bargalló N, Olondo L, Garcia AI, Capurro S, Caral L, Rumia J. Functional analysis of third ventriculostomy patency by quantification of CSF stroke volume by using cine phase-contrast MR imaging. *AJNR Am J Neuroradiol* 2005;26:2514–21.
- [21] Di X, Ragab M, Luciano MG. Cine phase-contrast MR images failed to predict clinical outcome following ETV. *Can J Neurol Sci* 2009;36:643–7.